

1 **Missing earthquake data reconstruction in the**
2 **space-time-magnitude domain**

3 **Angela Stallone^{1*}, and Giuseppe Falcone¹**

4 ¹Istituto Nazionale di Geofisica e Vulcanologia (INGV)

5 **Key Points:**

- 6 • A new Python toolbox for the replenishment of incomplete seismic catalogs is de-
7 veloped
8 • The code is freely-available, data-driven and minimizes the users' inputs
9 • Numerical and real-case tests are provided

*Via di Vigna Murata, 605 - 00143 Rome, Italy

Corresponding author: Angela Stallone, angela.stallone@ingv.it

Abstract

Short term aftershock incompleteness (STAI) can strongly bias any analysis built on the assumption that seismic catalogs have a complete record of events. Despite several attempts to tackle this issue, we are far from trusting any dataset in the immediate future of a large shock occurrence. Here we introduce RESTORE (REal catalogs STOchastic REplenishment), a Python toolbox implementing a stochastic gap-filling method, which automatically detects the STAI gaps and reconstructs the missing events in the space-time-magnitude domain. The algorithm is based on empirical earthquake properties and relies on a minimal number of assumptions about the data. Through a numerical test, we show that RESTORE returns an accurate estimation of the number of missed events and correctly reconstructs their magnitude, location and occurrence time. We also conduct a real-case test, by applying the algorithm to the M_W 6.2 Amatrice aftershocks sequence. The STAI-induced gaps are filled and missed earthquakes are restored in a way which is consistent with data. RESTORE, which is made freely available, is a powerful tool to tackle the STAI issue, and will hopefully help to implement more robust analyses for advancing operational earthquake forecasting and seismic hazard assessment.

1 Introduction

It is well known that analyzing an incomplete seismic catalog could severely bias studies aimed to: 1) estimate the Gutenberg-Richter parameters, their uncertainty, together with their variation in space and/or time (e.g. Knopoff et al., 1982; Schorlemmer et al., 2003; Woessner & Wiemer, 2005; Mignan & Woessner, 2012b; Marzocchi et al., 2020); 2) estimate the Epidemic-Type Aftershock Sequence (ETAS model: Ogata, 1988, 1998) parameters by maximum-likelihood techniques (Helmstetter et al., 2005, 2006; Hainzl et al., 2013; Omi et al., 2014; Seif et al., 2017; Zhuang et al., 2017); 3) perform a statistical analysis of earthquake data (e.g. Helmstetter et al., 2006; Christophersen & Smith, 2008; Iwata, 2008; Brodsky, 2011; Felzer et al., 2015; Stallone & Marzocchi, 2019).

The first two types of studies, in particular, have application in operational earthquake forecasting and seismic hazard assessment (Woessner et al., 2015), this implying that complete recording of seismic events is of primary importance in any analysis of this kind. Unfortunately, a careful estimation of the magnitude of completeness M_c is a necessary but not sufficient condition for a robust seismicity analysis. As a matter of fact, temporal changes in M_c can occur, mainly due to short term aftershock incompleteness (STAI from now on) (Ogata & Katsura, 1993; Kagan, 2004; Mignan & Woessner, 2012b; Omi et al., 2013), which arise from the under-reporting of small events after large earthquakes. These fluctuations, although transient, can severely alter the final results. For instance, (Zhuang et al., 2017) demonstrate how severe can be the influence of short-term missing aftershocks on the estimation of the ETAS parameter α (which is linked to earthquakes triggering capability). A solution to this issue would be improving the detection of early aftershocks of a large earthquake. This is possible by implementing waveform-based techniques (Peng et al., 2006, 2007; Enescu et al., 2007, 2009; Peng & Zhao, 2009). However, even in these cases, the detection capability of the missing events is far from being optimal. A quick fix could be to draw out earthquakes occurred after a large shock, for as long as the time required to the magnitude of completeness to return to the average value estimated for the whole catalog. Alternatively, one could model the magnitude of completeness as a function of time $M_c(t)$ and keep only those events whose magnitude is $\geq M_c(t)$ (e.g. Helmstetter et al., 2006; Lippiello et al., 2012). However, these approaches are not trivial, since they rely on user-defined criteria for identifying the critical events to be removed. Furthermore, a cut-and-run strategy could yield to a severe diminishment of the analyzed data, which is not always desirable. More recently, (Zhuang et al., 2017, 2019) have proposed a stochastic algorithm to replenish the portions of a seismic catalog where smaller events are missing. This approach is based on empirical

distribution functions estimated for the range of data where the catalog can be considered complete. However, it cannot be easily extended to the spatial domain and the detection of the missing area is not fully automated. Here we present RESTORE, a Python toolbox based on a stochastic gap-filling method, which reconstructs missing events in the space-time-magnitude domain and implements an automatized recognition of the critical regions with missing events (no input required from the user).

2 The algorithm

RESTORE allows to generate time, location and magnitude of those earthquakes that have not been detected by the seismic network due to the overlap of earthquake signals in seismic records after the occurrence of a large earthquake. Given the transient characteristic of STAI, the replenishment of missing data only pertains to limited portions of the catalog, i.e. those being affected by the occurrence of a large event. First, the temporal variability of M_c is assessed by means of a sliding overlapping windows approach, which collects estimates of M_c at the end of each window. Since the window has a fixed number of events k and its shift δk is constant, estimates of M_c are elapsed by δk events. The algorithm implements a statistic-based approach to pinpoint those time intervals where a threshold value for the magnitude of completeness M_c^* is significantly exceeded ("STAI gaps" from now on). For each interval, fluctuations in the completeness magnitude, represented by the δk -shifted moving-window estimates of M_c , are accounted for to reconstruct the missing earthquakes: the higher the estimated M_c , the higher the number of earthquakes to be replenished. It follows that the moving-window approach is functional for both the identification of STAI gaps and for their discretization. The latter is essential for a high-resolution temporal reconstruction of M_c inside the STAI gaps. The number of missing events within each δk -step is estimated by calculating the difference between the observed counts and the counts predicted by the Gutenberg-Richter relationship. Magnitude, occurrence time and location of the simulated events are reconstructed implementing Monte Carlo sampling techniques. More specifically, magnitudes are randomly sampled from the Gutenberg-Richter's law, bounded between the reference value M_c^* and the value within the δk -step. Occurrence times are simulated from an uniform distribution whose support are the time limits of the δk -step. The latter is based on the assumption that earthquake detection rate can be assumed constant within intervals including few events, i.e within very short time intervals. In other words, the probability of missing events within a δk -step can be considered time-independent if the step width is much shorter than the whole STAI gap width. As regards the spatial information, latitude and longitude of missing events are assigned with a probability that increases as the average rate of earthquake increases, the latter being derived from a Gaussian smoothing kernel. In the following, we examine the algorithm steps in more detail.

2.1 Query user inputs

The user is required to load the catalog as a csv file, in ZMAP format (i.e., Longitude, Latitude, Year, Month, Day, Magnitude, Depth, Hour, Minute, Second). Alternatively, he/she can download it from web services based on FDSN specification, by providing the parameters listed in Table 1, left column. There are two main requirements: 1) the magnitude type in the seismic catalog must be Mw (a bin size of 0.1 is assumed by default); 2) the catalog should include a period of seismic quiescence before the onset of one or more relatively strong seismic sequences. This is necessary for the estimation of the reference value for the magnitude of completeness (M_c^*), which needs not to be affected by STAI. For an unbiased estimation of M_c^* we recommend to include at least 1000 events in the seismic quiescent period. The parameters that need to be set for running RESTORE are reported in Table 1, right column. They will be explained in more detail in the subsequent sections.

Table 1. RESTORE input parameters^a.

| CATALOG PARAMETERS (optional) | INPUT PARAMETERS |
|-------------------------------|---------------------------|
| Minimum magnitude | Minimum magnitude |
| Minimum longitude | Moving-window size |
| Maximum longitude | Moving-window step |
| Minimum latitude | Spatial map domain limits |
| Maximum latitude | t_{seq} |
| Maximum depth | b -value |
| t_{start} | |
| t_{end} | |

^aLeft: catalog parameters (to be provided only when downloading the catalog from web services based on FDSN specification) - t_{start} : string representing the start time of the catalog in a recognizably valid format; t_{end} : string representing the end time of the catalog in a recognizably valid format.

Right: RESTORE parameters - t_{seq} : starting time of the seismic sequence (i.e., end of the seismic quiescent period).

113

2.2 Reference value for the magnitude of completeness

114

115

116

117

118

119

120

121

The reference value M_c^* must be evaluated for the seismically quiescent period preceding the onset of one or more relatively strong seismic sequences. It is estimated as the first magnitude value such that the hypothesis of exponentially-distributed data cannot be rejected at a significance level α (Lilliefors test, Lilliefors, 1969; Clauset et al., 2009). By default, $\alpha = 0.05$, but different values can be assigned. Alternatively, the user could input his/her own value for M_c^* , based on a priori information. The bootstrap method is implemented to estimate the uncertainty σ about the estimate of M_c^* returned by the Lilliefors test.

122

2.3 Temporal variations in M_c

123

124

125

126

127

128

129

130

131

132

133

134

135

RESTORE implements a moving window approach to analyze the variation of the magnitude of completeness as a function of time. By default, the window size is $k = 1000$ events (following Mignan & Woessner, 2012a), but it could be increased or decreased, depending on both the catalog size and the resolution the user needs to achieve. Intuitively, a small window highlights short-term variation in M_c , but it could return a biased estimate of M_c if the sample size is too small (due to the decreased power of the Lilliefors test); on the contrary, a larger window returns a faster and more robust estimate of M_c , but it is less sensitive to its transient fluctuations. The window is shifted by a step of δk events. By default, $\delta k = 250$ (following Mignan & Woessner, 2012a). The same considerations made for a larger/smaller window apply for a larger/smaller step. M_c is estimated by means of the Lilliefors test and its values are collected at the end of each window. Since the window has a fixed number of events k and its shift δk is constant, estimates of M_c are elapsed by δk events.

136

2.4 Automatic detection of STAI gaps

137

138

139

140

141

STAI gaps are identified as those where $M_c \geq M_c^* + 2\sigma$, i.e. where M_c is significantly larger than the reference value. The onset time of each gap is set equal to the time of the largest earthquake in the first step. Intuitively, it is the one responsible for the raise of the magnitude of completeness among the δk events. The end time of each gap is coincident with the occurrence time of the last event in the last step. In order to ac-

142 count for statistical fluctuations of the magnitude of completeness, small gaps - defined
 143 as those with a number of events $< 2 * \delta k$ - are removed.

144 2.5 Simulation of missing earthquakes

145 For a given STAI gap, the algorithm stores as many M_c estimates as the number
 146 of δk -steps in the gap. This information is used to evaluate the expected number of miss-
 147 ing events at the step level by means of the following formula (derived from the Gutenberg-
 148 Richter frequency-magnitude relationship):

$$N(M_c^* \leq M < M_c^S) = N(M \geq M_c^S) * 10^{b*n*mbin} - N(M \geq M_c^S), \quad (1)$$

149 where $N(M \geq M_c^S)$ is the observed number of events with a magnitude $\geq M_c^S$,
 150 the M_c value within the step, b represents the b -value estimated for the whole catalog,
 151 n is the number of magnitude bins, $mbin$ is the magnitude bin (usually $mbin = 0.1$).
 152 We refer to Appendix 1 for the derivation of Equation 1.

153 2.5.1 Simulation of magnitudes

154 Within each δk -step, the algorithm performs an iterative random sampling from
 155 the Gutenberg-Richter frequency-magnitude relationship, bounded between M_c^* and M_c^S .
 156 This is done by means of the inverse method (Devroye, 1986). The main steps are sum-
 157 marized in Algorithm 1.

Algorithm 1: Magnitude simulation

```

1  for each STAI gap do
2  |   for each step in the gap do
3  |   |   while count  $\leq$  Number of earthquakes missing in the step do
4  |   |   |   U = RAND(0,1);
5  |   |   |   M =  $(-1/b * \log(U) + M_c^* - mbin/2) * 10/10$ ;
6  |   |   |   if  $M \leq M_c^S$  then
7  |   |   |   |   keep M;
8  |   |   |   |   count + = 1;
9  |   |   |   else
10 |   |   |   |   reject M ;
11 |   |   |   |   count + = 0;
12 |   |   |   end
13 |   |   end
14 |   end
15 end
```

159 2.5.2 Simulation of occurrence times

160 Occurrence times are simulated from an uniform distribution whose support are
 161 the time limits of the δk -step. As already discussed, earthquake detection rate can be
 162 assumed constant within intervals including few events, i.e within very short time inter-
 163 vals. The main steps are summarized in Algorithm 2.

Algorithm 2: Occurrence times simulation

```

1 for each STAI gap do
2   for each step in the gap do
3     while count  $\leq$  Number of earthquakes missing in the step do
4        $t_{i-1}$  = start time of the step;
5        $t_i$  = end time of the step;
6       U = RAND(0,1);
7        $T = t_{i-1} + U * (t_i - t_{i-1})$ ;
8       count + = 1;
9     end
10  end
11 end

```

2.5.3 Simulation of epicenter coordinates

Latitude and longitude of missing events are assigned with a probability that increases as the rate of earthquakes increases, i.e. as the distance from the large event diminishes. The rationale is based on kernel smoothing techniques, commonly implemented to forecast the density of future seismicity given the spatial distribution of past events (e.g. Frankel, 1995; Helmstetter et al., 2006; Zechar & Jordan, 2010). Specifically, a Gaussian kernel (Zechar & Jordan, 2010) is used, which is a function of the smoothing distance σ only.

For each STAI gap, RESTORE extracts the pertaining subset from the catalog, that is all the events meeting the following two criteria: 1) their occurrence times range between the start and end time of the STAI gap; 2) their epicenter coordinates fall within a rectangular grid representing the large shock "influence area". As a proxy for the latter, the algorithm uses the estimation of the subsurface rupture length through the relation proposed by (Mai & Beroza, 2000):

$$M_o = 10^{\frac{3}{2} * (M_w + 10.7)} * 10^{-7}; \quad (2)$$

$$R_l = 10^{-5.20 + 0.35 * \log(M_o)} \quad (3)$$

The grid is discretized in cells, whose width depends on the bin in the latitude and longitude direction *sbin* (*sbin* = 0.01 deg in both the directions, by default). The smoothing kernel is defined as follow:

$$K_\sigma = \frac{1}{2\pi\sigma^2} \exp\left(\frac{-R^2}{2\sigma^2}\right), \quad (4)$$

where σ is the smoothing distance (set to 1 by default) and R is the distance of a given earthquake from a given grid node. The kernel smoothing technique offers an intuitive representation of seismicity clustering in space: as a matter of fact, events that are close in space will mainly contribute to the same (few) nodes in the grid. The events count at each grid node is estimated by summing up the contributions from all the events in the grid to that specific point. Normalizing the smoothed rate by the total rate yields the expected earthquake density over all the grid nodes. The latter is used as the basis for assigning epicenter locations to a given grid point, i.e. with a probability that is proportional to the expected earthquake rate at that location. This is achieved by simply applying the discrete version of the inverse method to the cumulative distribution of the normalized smoothed rate. Once an epicenter has been linked to a specific grid

193 point XY , its latitude (longitude) is simulated from an uniform distribution whose sup-
 194 port is $([lat(XY) - sbin, lat(XY) + sbin] [lon(XY) - sbin, lon(XY) + sbin])$. Main
 195 steps are summarized in Algorithm 3:

Algorithm 3: Epicenters latitude and longitudes simulation

```

input: CUMSUM: Cumulative sum of the (sorted) smoothed rate
1 for each STAI gap do
2   while count  $\leq$  Number of earthquakes missing in the STAI gap do
3     U = RAND(0,1);
4     for each grid point XY do
5       if CUMSUM(XY - 1)  $\leq$  U < CUMSUM(XY) then
6         U2 = RAND(0,1);
7         LON = LON(XY - 1) + U2 * sbin;
8         LAT = LAT(XY - 1) + U2 * sbin;
9       end
10    end
11    count + = 1;
12  end
13 end

```

197 **2.6 Output**

198 RESTORE replenishes the original catalog with the reconstructed events, by prop-
 199 erly taking into account the occurrence time of the latter. The resulting catalog is saved
 200 in ZMAP format and differs from the original one only for two aspects: 1) the depth col-
 201 umn is now a zeros vector, as this information has not been taken into account for the
 202 spatial simulation of missing earthquakes; 2) there is an additional column which flags
 203 events to 0 or 1, depending on whether they belong to the original catalog or they have
 204 been simulated. Additionally, several graphical outputs are returned:

- 205 • Time evolution of magnitude of completeness, with highlighted all detected STAI
- 206 gaps (the plot neglects the seismic quiescent period);
- 207 • Magnitudes versus sequential numbers for the original and replenished catalogs:
- 208 this is a great, tough qualitative, tool to highlight STAI issues which could pos-
- 209 sible affect earthquake magnitudes through time;
- 210 • Magnitude versus time for 1) the original catalog and the reconstructed events;
- 211 2) the original catalog only;
- 212 • Spatial map of the original events with overlapping reconstructed events;
- 213 • Magnitude-frequency distribution (MFD) for both the original and the replenished
- 214 catalogs.

215 Finally, the magnitude of completeness is estimated by the Lilliefors test for both
 216 the original and the replenished catalogs. This provides an additional test for validat-
 217 ing the outputs by RESTORE: intuitively, we expect the M_c estimated for the replen-
 218 ished catalog to be very close to the pre-sequence value M_c^* . However, the user should
 219 keep in mind that the statistical power of the Lilliefors test (and, more in general, of
 220 the Kolmogorov-Smirnov test) greatly increases with the sample size (Stallone, 2018; Mar-
 221 zocchi et al., 2020). It follows that for a large number of events, which can be the case
 222 for the replenished catalog, the Lilliefors test becomes very sensitive to even slight de-
 223 viations from an exponential distribution. This is not necessary ideal, since the detected
 224 departures could actually arise from magnitude errors. We therefore strongly recommend
 225 to inspect the replenished catalog by both the Lilliefors test and the outputs listed above.

226 3 Synthetic test

227 As a validation test, we implement numerical modeling, which enables us to control
 228 the number of missing events and their collocation in the magnitude-time-space do-
 229 main. The goal is to check whether the algorithm is capable of reconstructing this in-
 230 formation with an acceptable degree of accuracy. First, we simulate a seismic catalog
 231 by implementing the stochastic program described in (Felzer et al., 2002), which sim-
 232 ulates the ETAS model (Ogata, 1988) as a branching process. In the original code, earth-
 233 quakes with a magnitude larger than 6.5 are modeled as planar sources. We change that
 234 by modeling all the events as point sources. We use the program to simulate a 2-years-
 235 long catalog in Southern California, with magnitudes ranging from 2 to 6.9. We leave
 236 unchanged the remaining parameters needed for the simulation as indicated in the code.
 237 The b -value is set equal to 1. Since our next step is to simulate incompleteness of after-
 238 shocks following the largest earthquake in the catalog, we select a subset of the simu-
 239 lated dataset, which ranges from 1 year before to 3 months after the occurrence of the
 240 largest earthquake ($M = 6.9$). After this step, the original catalog includes 11,169 events.

241 We simulate the STAI issue for the largest event by following the approach described
 242 in (Ogata & Katsura, 2006). Specifically, earthquakes are filtered out at a magnitude-
 243 dependent rate, according to the cumulative normal distribution:

$$F(M|\mu, \sigma) = \int_{-\infty}^M \frac{1}{\sqrt{2\pi}\sigma} e^{-\frac{(x-\mu)^2}{2\sigma^2}} dx, \quad (5)$$

244 where μ and σ are constant: the first is the magnitude with a detection rate of 50%;
 245 the latter is the standard deviation of the normal distribution. $F(M|\mu, \sigma)$ is the prob-
 246 ability of detection at magnitude M . See (Stallone, 2018) for more details. For our sim-
 247 ulations, we set $\mu = 3$ and $\sigma = 0.2$; we assume that the magnitude of completeness is
 248 restored to the reference value 3 days after the occurrence of the large event. The cat-
 249 alog after STAI modeling includes 7,744 events.

250 Figure 1 shows the frequency-magnitude distribution for the original (left) and in-
 251 complete (right) catalog, for which the STAI issue has been modeled. Figure 2 plots the
 252 magnitude of events as a function of time (over a period of 0-3 days from the mainshock)
 253 for the original (top) and incomplete (bottom) catalog.

254 As a next step, we implement RESTORE for reconstructing the missing events in
 255 the magnitude-time-space domain. We leave the default values for the window size (1000
 256 events) and the step (250). The reference value for the magnitude of completeness equals
 257 the minimum magnitude in the synthetic catalog, i.e. 2.0. We set the b -value for the Gutenberg-
 258 Richter law to 1. Figure 3 shows some of the graphical outputs returned by the algorithm.
 259 We observe that occurrence times, magnitude range and locations of missing events have
 260 been correctly reconstructed. The replenished catalog includes 11,106 events, i.e. the
 261 number of missing earthquakes is correct within an acceptable error bound (1.8%). The
 262 magnitude of completeness estimated by the Lilliefors test is 2.8 and 2.1 for the incom-
 263 plete and replenished catalog, respectively.

264 In order to further inspect the algorithm performance, we compare the frequency-
 265 magnitude distribution and the magnitude-time plot (this latter within 3 days from the
 266 large shock) for 1) the original synthetic catalog before STAI modeling; 2) the original
 267 synthetic catalog after STAI modeling; 3) the replenished catalog. Results are shown in
 268 Figure 4 and Figure 5. This comparison further proves the good performance of the al-
 269 gorithm when reconstructing missing events in the magnitude-time-space domain.

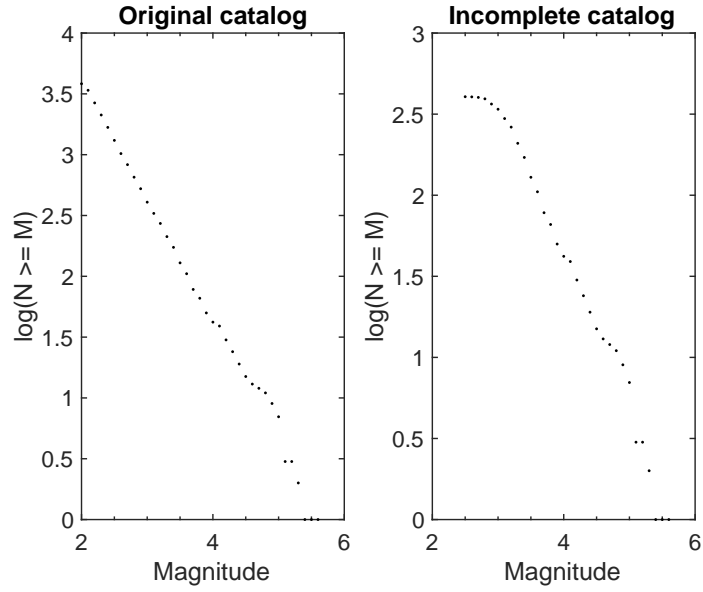


Figure 1. Frequency-magnitude distribution for the original synthetic catalog before STAI modeling (left) and after STAI modeling (right).

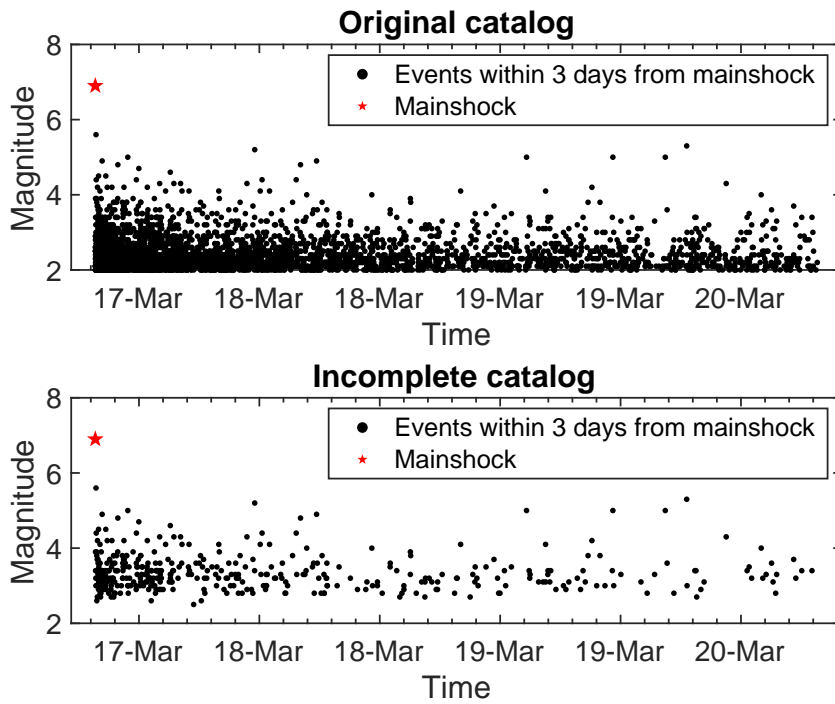


Figure 2. Magnitude-time plot for events occurred within 3 days from the large shock. Top: before STAI modeling. Bottom: after STAI modeling.

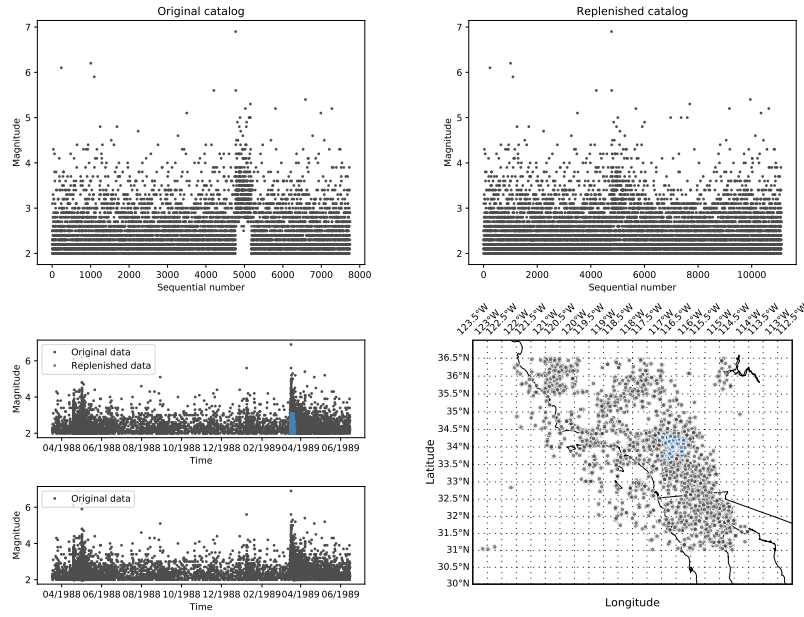


Figure 3. Main graphical outputs of the algorithm. Top Left: Magnitudes versus sequential numbers for the original (synthetic) catalog; Top Right: Magnitudes versus sequential numbers for the replenished catalog; Bottom Left: Magnitude versus time for 1) the original catalog and the reconstructed events 2) the original catalog only; Bottom Right: Spatial map of the original events with overlapping reconstructed events.

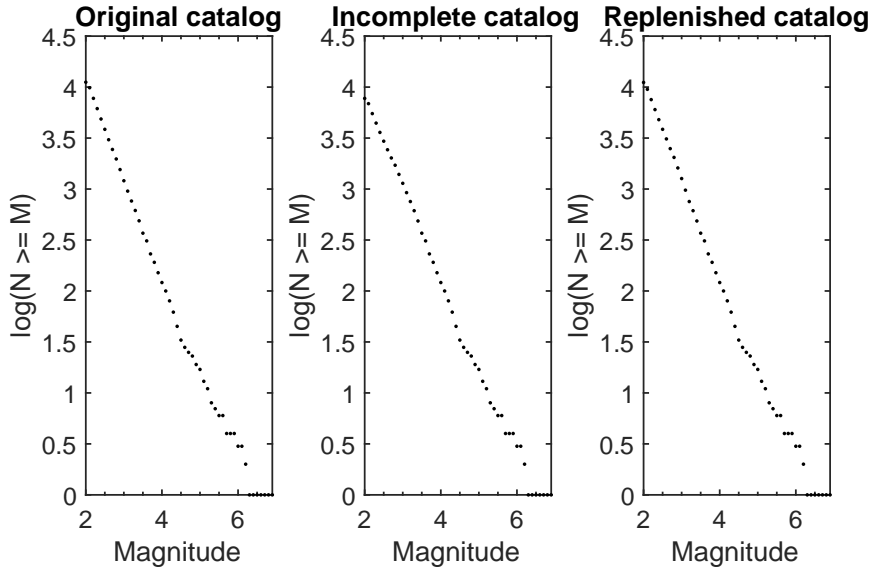


Figure 4. Frequency-magnitude distribution. From left to right: original synthetic catalog before STAI modeling, original synthetic catalog after STAI modeling, replenished catalog.

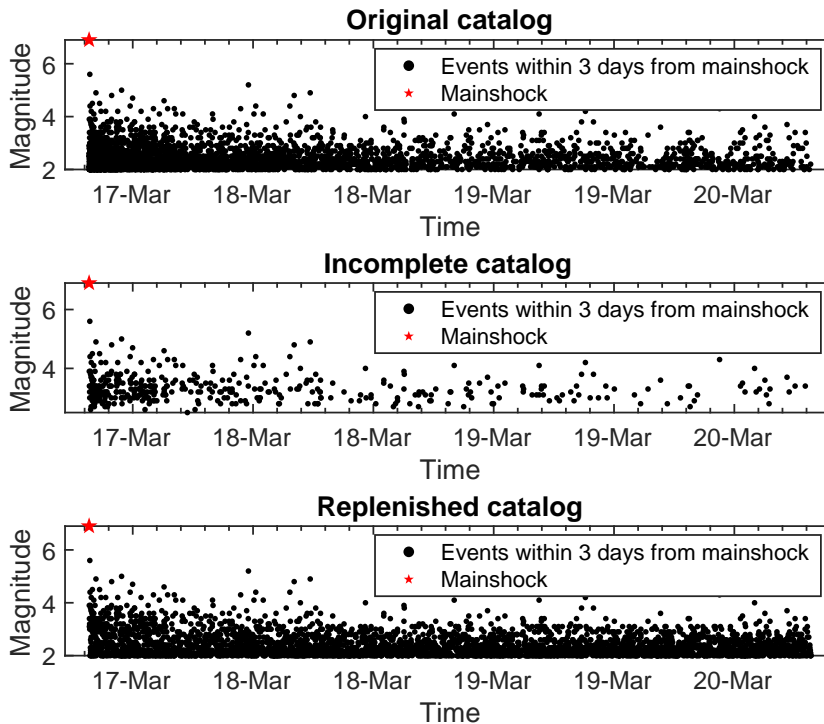


Figure 5. Magnitude-time plot. From top to bottom: original synthetic catalog before STAI modeling, original synthetic catalog after STAI modeling, replenished catalog.

270 4 Real-case test (Amatrice earthquake)

271 We apply RESTORE to the 24 August 2016 Mw 6.2 Amatrice earthquake. The
 272 downloaded catalog covers the period from 1st January 2016 to 30 September 2016 and
 273 includes 18,623 events. We leave the default values for the window size (1000 events) and
 274 the step (250). The seismically quiescent period ranges from 1st January 2016 to 24 Au-
 275 gust 2016 and includes 2,351 events. We estimate the reference value for the magnitude
 276 of completeness M_c^* with the Lilliefors test provided by the algorithm, which returns $M_c^* =$
 277 1.2. This leaves 13,120 earthquakes with $M \geq M_c^*$. Finally, we set the b -value for the
 278 Gutenberg-Richter law equal to 1. The replenished catalog includes 22,470 events. Fig-
 279 ure 6 plots the magnitude of completeness as a function of time, with highlighted the
 280 detected STAI gaps (four in this case). The magnitude of completeness is recovered to
 281 the reference value M_c^* after about 1 month. Figure 7 shows the other graphical outputs
 282 returned by the algorithm. While the ground truth is not known in the real-case test,
 283 we observe that the missing events are correctly reconstructed in a way which is consis-
 284 tent with data.

285 5 Conclusions

286 We have presented RESTORE, a new Python toolbox for the reconstruction of mag-
 287 nitude, time and location of missed events in the coda of large shocks. It relies on very
 288 few assumptions - e.g. the detection rate of events can be assumed to be constant within
 289 periods of time that are much shorter than the STAI extent. It also relies on a data-driven
 290 approach, which is built on well-known empirical properties of earthquake data, such as
 291 the Gutenberg-Richter law for the frequency-magnitude distribution and the aftershocks

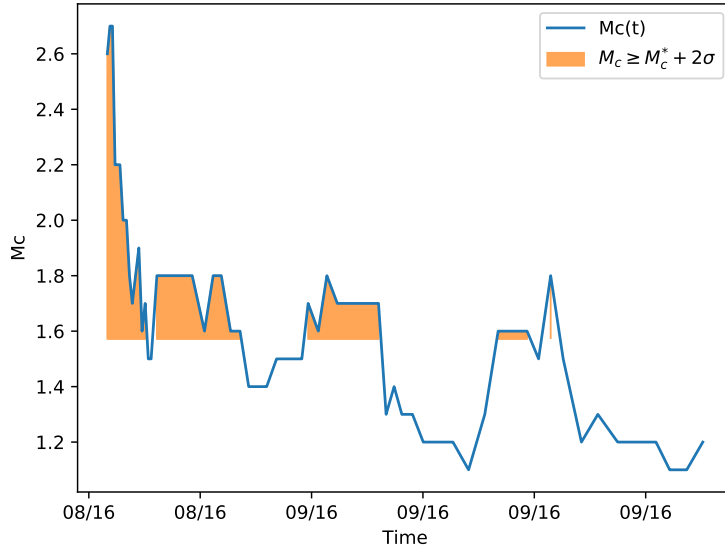


Figure 6. Temporal evolution of the magnitude of completeness, with highlighted the detected STAI gaps. The moving-window includes 1000 events and is shifted by 250 events.

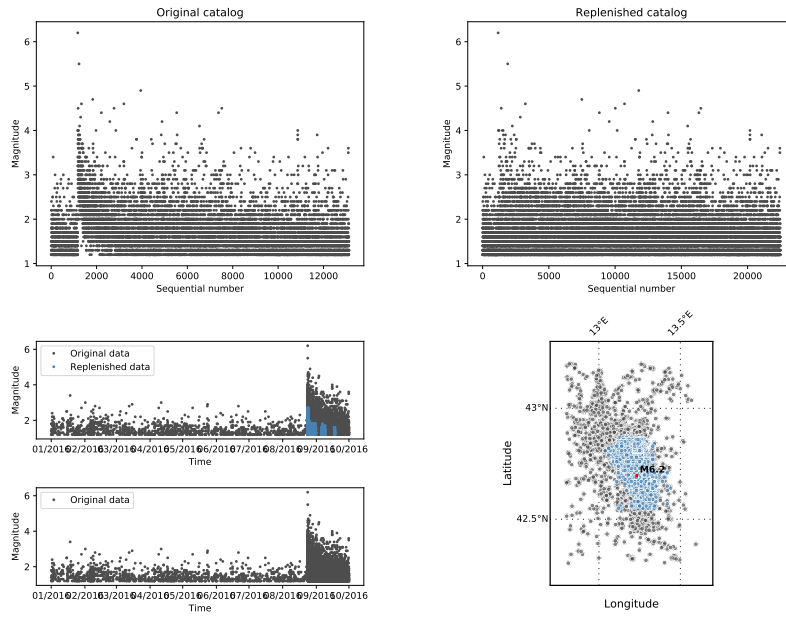


Figure 7. Main graphical outputs of the algorithm. Top Left: Magnitudes versus sequential numbers for the original catalog; Top Right: Magnitudes versus sequential numbers for the replenished catalog; Bottom Left: Magnitude versus time for 1) the original catalog and the reconstructed events 2) the original catalog only; Bottom Right: Spatial map of the original events with overlapping reconstructed events.

292 clustering in space. The critical subsets of the catalog that are affected by STAI are au-
 293 tomatically detected through a moving-window approach, which identifies statistically
 294 significant departures of the magnitude of completeness with respect to a reference value.
 295 We demonstrate the robustness of the algorithm by means of a numerical and a real-case
 296 test. In the first case, the ground truth is accurately recovered: not only the number of
 297 missing earthquakes is correctly retrieved, but their space-time-magnitude stochastic dis-
 298 tribution is correctly resolved as well. The real-test case, which applies to the Mw 6.2
 299 Amatrice earthquake, further proves the good performance of the algorithm, which re-
 300 constructs the missed events in a way that is consistent with the data. RESTORE is made
 301 freely available and can be downloaded at the link provided in the Acknowledgments.
 302 It promises to become a valuable research tool to tackle the STAI issue, which can severely
 303 bias any study based on the analysis of real seismic catalogs. Hopefully, it will help re-
 304 ducing these sources of bias, thus leading to better operational earthquake forecasting
 305 and seismic hazard assessment.

306 6 Data Availability Statement

307 The algorithm RESTORE is available at the following Zenodo repository: <https://doi.org/10.5281/zenodo.3952182>, and can also be downloaded from GitHub at this
 308 link: <https://github.com/angystallone/RESTORE>. The repository includes the dataset
 309 used for the synthetic test as well. The seismic catalog used for the real-case test (Am-
 310 atrice earthquake) is the HOMogenized instrUMENTal Seismic catalog (HORUS) of Italy
 311 (Lolli et al., 2020) and it can be downloaded at this link: <https://horus.bo.ingv.it/>.
 312

313 Acknowledgments

314 This project has been funded by the Seismic Hazard Center (Centro di Pericolosità
 315 Sismica, CPS, at the Istituto Nazionale di Geofisica e Vulcanologia, INGV).

316 Appendix A Calculation of number of missing events

317 Here we derive Equation 1 of the text. The frequency-magnitude distribution of
 318 earthquakes is typically described by the Gutenberg-Richter (G-R) exponential law (Gutenberg
 319 & Richter, 1944):

$$N(M) = 10^{a-b*M}, \quad (\text{A1})$$

320 where $N(M)$ is the number of events with magnitude $\geq M$ ($M \geq M_{min}$, i.e. the
 321 minimum magnitude in the earthquake catalog), a is a constant related to the total seis-
 322 mic rate and b is the b -value, controlling the relative number of large earthquakes in the
 323 catalog.

324 Let us consider the case where $M_2 \geq M_1$. We have:

$$\begin{aligned} N(M \geq M_1) &= 10^{a-b*M_1} \\ N(M \geq M_2) &= 10^{a-b*M_2} \end{aligned}$$

325 When considering the whole catalog, the number of expected events with magni-
 326 tude M , $M_1 \leq M < M_2$ is simply given by $N(M \geq M_1) - N(M \geq M_2)$.

327 However, when considering a subset of the catalog, we need to rescale our prob-
 328 lem (in other words, we need to get rid of the term 10^a).

329 We start by expressing $N(M \geq M_1)$ as a function of $N(M \geq M_2)$ and b only,
 330 by calculating their ratio:

$$\frac{N(M \geq M_1)}{N(M \geq M_2)} = 10^{-b*(M_1-M_2)} \quad (\text{A2})$$

331 It follows that:

$$N(M \geq M_1) = N(M \geq M_2) * 10^{-b*(M_1-M_2)} \quad (\text{A3})$$

332 We observe that $M_2 = M_1 + n * mbin$, where $mbin$ is the magnitude binning (usu-
333 ally equal to 0.1). It follows that:

$$N(M \geq M_1) = N(M \geq M_2) * 10^{b*n*mbin} \quad (\text{A4})$$

334 This simple relationship allows us to write the number of expected events with mag-
335 nitude M , $M_1 \leq M < M_2$, as a function of the number of events with magnitude M , $M \geq$
336 M_2 , observed in the catalog subset:

$$N(M_1 \leq M < M_2) = N(M \geq M_2) * 10^{b*n*mbin} - N(M \geq M_2) \quad (\text{A5})$$

337 This enables us to extrapolate the frequency of earthquakes above a given magni-
338 tude to any lower magnitude cutoff. We implicitly assume that the b -value is constant
339 for any subset of the whole catalog.

340 References

- 341 Brodsky, E. (2011). The spatial density of foreshocks. *Geophysical Research Letters*,
342 *38*(10).
- 343 Christophersen, A., & Smith, E. G. (2008). Foreshock rates from aftershock abun-
344 dance. *Bulletin of the Seismological Society of America*, *98*(5), 2133–2148.
- 345 Clauset, A., Shalizi, C. R., & Newman, M. E. (2009). Power-law distributions in em-
346 pirical data. *SIAM review*, *51*(4), 661–703.
- 347 Devroye, L. (1986). Sample-based non-uniform random variate generation. In *Pro-*
348 *ceedings of the 18th conference on winter simulation* (pp. 260–265).
- 349 Enescu, B., Mori, J., & Miyazawa, M. (2007). Quantifying early aftershock activity
350 of the 2004 mid-niigata prefecture earthquake (mw6. 6). *Journal of Geophys-*
351 *ical Research: Solid Earth*, *112*(B4).
- 352 Enescu, B., Mori, J., Miyazawa, M., & Kano, Y. (2009). Omori-utsu law c-values as-
353 sociated with recent moderate earthquakes in japan. *Bulletin of the Seismolog-*
354 *ical Society of America*, *99*(2A), 884–891.
- 355 Felzer, K. R., Becker, T. W., Abercrombie, R. E., Ekström, G., & Rice, J. R. (2002).
356 Triggering of the 1999 mw 7.1 hector mine earthquake by aftershocks of the
357 1992 mw 7.3 landers earthquake. *Journal of Geophysical Research: Solid*
358 *Earth*, *107*(B9), ESE–6.
- 359 Felzer, K. R., Page, M. T., & Michael, A. J. (2015). Artificial seismic acceleration.
360 *Nature Geoscience*, *8*(2), 82–83.
- 361 Frankel, A. (1995). Mapping seismic hazard in the central and eastern united states.
362 *Seismological Research Letters*, *66*(4), 8–21.
- 363 Gutenberg, B., & Richter, C. F. (1944). Frequency of earthquakes in california. *Bul-*
364 *letin of the Seismological Society of America*, *34*(4), 185–188.
- 365 Hainzl, S., Zakharova, O., & Marsan, D. (2013). Impact of aseismic transients on the
366 estimation of aftershock productivity parameters. *Bulletin of the Seismological*
367 *Society of America*, *103*(3), 1723–1732.

- 368 Helmstetter, A., Kagan, Y. Y., & Jackson, D. D. (2005). Importance of small earth-
 369 quakes for stress transfers and earthquake triggering. *Journal of Geophysical*
 370 *Research: Solid Earth*, *110*(B5).
- 371 Helmstetter, A., Kagan, Y. Y., & Jackson, D. D. (2006). Comparison of short-term
 372 and time-independent earthquake forecast models for southern california. *Bul-*
 373 *letin of the Seismological Society of America*, *96*(1), 90–106.
- 374 Iwata, T. (2008). Low detection capability of global earthquakes after the occurrence
 375 of large earthquakes: Investigation of the harvard cmt catalogue. *Geophysical*
 376 *Journal International*, *174*(3), 849–856.
- 377 Kagan, Y. Y. (2004). Short-term properties of earthquake catalogs and models
 378 of earthquake source. *Bulletin of the Seismological Society of America*, *94*(4),
 379 1207–1228.
- 380 Knopoff, L., Kagan, Y. Y., & Knopoff, R. (1982). b values for foreshocks and after-
 381 shocks in real and simulated earthquake sequences. *Bulletin of the Seismologi-*
 382 *cal Society of America*, *72*(5), 1663–1676.
- 383 Lilliefors, H. W. (1969). On the kolmogorov-smirnov test for the exponential dis-
 384 tribution with mean unknown. *Journal of the American Statistical Association*,
 385 *64*(325), 387–389.
- 386 Lippiello, E., Godano, C., & de Arcangelis, L. (2012). The earthquake magnitude is
 387 influenced by previous seismicity. *Geophysical Research Letters*, *39*(5).
- 388 Lolli, B., Randazzo, D., Vannucci, G., & Gasperini, P. (2020). The homogenized in-
 389 strumental seismic catalog (horus) of italy from 1960 to present. *Seismological*
 390 *Society of America*, *91*(6), 3208–3222.
- 391 Mai, P. M., & Beroza, G. C. (2000). Source scaling properties from finite-fault-
 392 rupture models. *Bulletin of the Seismological Society of America*, *90*(3), 604–
 393 615.
- 394 Marzocchi, W., Spassiani, I., Stallone, A., & Taroni, M. (2020). How to be fooled
 395 searching for significant variations of the b-value. *Geophysical Journal Interna-*
 396 *tional*, *220*(3), 1845–1856.
- 397 Mignan, A., & Woessner, J. (2012a). Estimating the magnitude of completeness
 398 for earthquake catalogs. *Community Online Resource for Statistical Seismicity*
 399 *Analysis*, 1–45.
- 400 Mignan, A., & Woessner, J. (2012b). *Theme iv—understanding seismicity cat-*
 401 *alogs and their problems* (Tech. Rep.). Technical Report doi: [https://doi.](https://doi.org/10.5078/corssa-00180805)
 402 [org/10.5078/corssa-00180805](https://doi.org/10.5078/corssa-00180805), Community . . .
- 403 Ogata, Y. (1988). Statistical models for earthquake occurrences and residual
 404 analysis for point processes. *Journal of the American Statistical association*,
 405 *83*(401), 9–27.
- 406 Ogata, Y. (1998). Space-time point-process models for earthquake occurrences. *An-*
 407 *nals of the Institute of Statistical Mathematics*, *50*(2), 379–402.
- 408 Ogata, Y., & Katsura, K. (1993). Analysis of temporal and spatial heterogeneity
 409 of magnitude frequency distribution inferred from earthquake catalogues. *Geo-*
 410 *physical Journal International*, *113*(3), 727–738.
- 411 Ogata, Y., & Katsura, K. (2006). Immediate and updated forecasting of aftershock
 412 hazard. *Geophysical research letters*, *33*(10).
- 413 Omi, T., Ogata, Y., Hirata, Y., & Aihara, K. (2013). Forecasting large aftershocks
 414 within one day after the main shock. *Scientific reports*, *3*, 2218.
- 415 Omi, T., Ogata, Y., Hirata, Y., & Aihara, K. (2014). Estimating the etas model
 416 from an early aftershock sequence. *Geophysical Research Letters*, *41*(3), 850–
 417 857.
- 418 Peng, Z., Vidale, J. E., & Houston, H. (2006). Anomalous early aftershock decay
 419 rate of the 2004 mw6. 0 parkfield, california, earthquake. *Geophysical Research*
 420 *Letters*, *33*(17).
- 421 Peng, Z., Vidale, J. E., Ishii, M., & Helmstetter, A. (2007). Seismicity rate imme-
 422 diately before and after main shock rupture from high-frequency waveforms in

- 423 japan. *Journal of Geophysical Research: Solid Earth*, 112(B3).
- 424 Peng, Z., & Zhao, P. (2009). Migration of early aftershocks following the 2004 park-
425 field earthquake. *Nature Geoscience*, 2(12), 877–881.
- 426 Schorlemmer, D., Neri, G., Wiemer, S., & Mostaccio, A. (2003). Stability and signif-
427 icance tests for b-value anomalies: Example from the tyrrhenian sea. *Geophys-
428 ical research letters*, 30(16).
- 429 Seif, S., Mignan, A., Zechar, J. D., Werner, M. J., & Wiemer, S. (2017). Estimating
430 etas: The effects of truncation, missing data, and model assumptions. *Journal
431 of Geophysical Research: Solid Earth*, 122(1), 449–469.
- 432 Stallone, A. (2018). *Statistical analysis of earthquake occurrences and implications
433 for earthquake forecasting and seismic hazard assessment* (Doctoral disserta-
434 tion, University of Roma TRE). doi: 10.13140/RG.2.2.35672.65282/1
- 435 Stallone, A., & Marzocchi, W. (2019). Empirical evaluation of the magnitude-
436 independence assumption. *Geophysical Journal International*, 216(2), 820–
437 839.
- 438 Woessner, J., Laurentiu, D., Giardini, D., Crowley, H., Cotton, F., Grünthal, G., . . .
439 others (2015). The 2013 european seismic hazard model: key components and
440 results. *Bulletin of Earthquake Engineering*, 13(12), 3553–3596.
- 441 Woessner, J., & Wiemer, S. (2005). Assessing the quality of earthquake catalogues:
442 Estimating the magnitude of completeness and its uncertainty. *Bulletin of the
443 Seismological Society of America*, 95(2), 684–698.
- 444 Zechar, J. D., & Jordan, T. H. (2010). Simple smoothed seismicity earthquake fore-
445 casts for italy. *Annals of Geophysics*, 53(3), 99–105.
- 446 Zhuang, J., Ogata, Y., & Wang, T. (2017). Data completeness of the kumamoto
447 earthquake sequence in the jma catalog and its influence on the estimation of
448 the etas parameters. *Earth, Planets and Space*, 69(1), 36.
- 449 Zhuang, J., Wang, T., & Koji, K. (2019). Detection and replenishment of missing
450 data in marked point processes.. Retrieved from [http://bemlar.ism.ac.jp/
451 zhuang/pubs/zhuang2019statsini.pdf](http://bemlar.ism.ac.jp/zhuang/pubs/zhuang2019statsini.pdf)